

## Antigen retrieval pre-treatment causes a different expression pattern of Ca<sub>v</sub>3.2 in rat and mouse spinal dorsal horn

Xiao E Cheng,<sup>1,2</sup> Long Xian Ma,<sup>2</sup>  
Xiao Jin Feng,<sup>1,2</sup> Meng Ye Zhu,<sup>3</sup>  
Da Ying Zhang,<sup>3</sup> Lin Lin Xu,<sup>1</sup> Tao Liu<sup>1</sup>

<sup>1</sup>Center for Experimental Medicine, the First Affiliated Hospital of Nanchang University

<sup>2</sup>Department of Anesthesiology, the First Affiliated Hospital of Nanchang University

<sup>3</sup>Department of Pain Clinic, the First Affiliated Hospital of Nanchang University, China

### Abstract

Ca<sub>v</sub>3 channels consist of three isoforms, Ca<sub>v</sub>3.1 (α1G), Ca<sub>v</sub>3.2 (α1H), and Ca<sub>v</sub>3.3 (α1I), which produce low-threshold spikes that trigger burst firings in nociceptive neurons of the spinal dorsal horn (SDH) and dorsal root ganglion (DRG). Although Ca<sub>v</sub>3.2 plays a crucial role in pathological pain, its distribution in SDH still remains controversial. One study showed that Ca<sub>v</sub>3.2 is ubiquitously expressed in neurons, but another study implied that Ca<sub>v</sub>3.2 is expressed restricted to astrocytes. To unravel these discrepancies, we used methods of immunohistochemistry either with or without antigen retrieval (AR) pre-treatment to detect Ca<sub>v</sub>3 in SDH and DRG from both rats and mice. Moreover, Ca<sub>v</sub>3.2 mRNA was detected in mice SDH using *in situ* hybridization. We found that the expression pattern of Ca<sub>v</sub>3.2 but not Ca<sub>v</sub>3.1 and Ca<sub>v</sub>3.3 in SDH were largely different with or without AR pre-treatment, which showed a neuron-like and an astrocyte-like appearance, respectively. Double staining further demonstrated that Ca<sub>v</sub>3.2 was mainly co-stained with the neuronal marker NeuN in the presence of AR but was with glial fibrillary acidic protein (GFAP, marker for astrocytes) in the absence of AR pre-treatment. Importantly, Ca<sub>v</sub>3.2 mRNA was mainly co-localized with Ca<sub>v</sub>3.2 but not GFAP. Together, our findings indicate that AR pre-treatment or not impacts the expression pattern of Ca<sub>v</sub>3.2, which may make a significant contribution to the future study of Ca<sub>v</sub>3.2 in SDH.

### Introduction

T-type (Ca<sub>v</sub>3) channels are low-voltage-activated (LVA) calcium channels that are encoded by three α1 subunit genes: α1G (Ca<sub>v</sub>3.1), α1H (Ca<sub>v</sub>3.2), and α1I (Ca<sub>v</sub>3.3),<sup>1</sup> which are widely distributed in brain, spinal cord and dorsal root ganglion (DRG).<sup>2</sup> Besides, immunohistochemical (IHC) studies have demonstrated that the proteins of Ca<sub>v</sub>3.1-3.3 are broadly expressed in the peripheral and central nervous system.<sup>3-7</sup> The role of Ca<sub>v</sub>3.2 in pathological pain has been extensively studied by behavioral, electrophysiological, and molecular biological methods during the last decade. For example, the Western blot immunoassay found that the expression of Ca<sub>v</sub>3.2 was increased in DRG and spinal dorsal horn (SDH) from rodents of cystitis-related bladder pain,<sup>8</sup> paclitaxel-induced peripheral neuropathy,<sup>9</sup> and loose ligatures of sciatic nerve induced neuropathic pain models,<sup>10</sup> *etc.* Moreover, T-type currents recorded in DRG were enhanced in various animal models of pathological pain.<sup>11</sup> Consistently, intrathecal injection of an antisense oligonucleotide (targeted to the α1-subunit of Ca<sub>v</sub>3.2, but not Ca<sub>v</sub>3.1 or Ca<sub>v</sub>3.3) or T-type channel blockers could alleviate pathological pain.<sup>12,13</sup> The above results suggest that Ca<sub>v</sub>3.2 plays a crucial role in the modulation of pathological pain. Therefore, it is important to identify the cell-type specific expression of Ca<sub>v</sub>3.2 channel in DRG and SDH. Up to now, the expression pattern of Ca<sub>v</sub>3.2 in DRG is consensus, that is, Ca<sub>v</sub>3.2 is mainly distributed in small- and medium-diameter DRG neurons.<sup>5,9,13-18</sup> However, in SDH, the expression pattern of Ca<sub>v</sub>3.2 is different. Chen *et al.* found that Ca<sub>v</sub>3.2 was restricted to the neurons but not microglia or astrocytes.<sup>5</sup> In contrast, Li *et al.* found that Ca<sub>v</sub>3.2 was co-localized to glial fibrillary acidic protein (GFAP)-positive cells (marker of astrocyte) but not NeuN- (marker of neuron) or OX42-positive (marker of microglia) cells.<sup>9</sup> One possible explanation for these differences might be that formaldehyde fixation compromises immunoreactivity of Ca<sub>v</sub>3.2 antigen by preventing contact between the epitopes and the antibodies, which will affect the outcome of an IHC staining.<sup>19,20</sup> To test this hypothesis, we investigated the IHC staining of Ca<sub>v</sub>3.2 in SDH and DRG sections with or without antigen retrieval (AR) pre-treatment which can unmask the antigens in formaldehyde-fixed tissue sections. The IHC staining of other two subtypes (Ca<sub>v</sub>3.1 and Ca<sub>v</sub>3.3) were also tested as well. To further determine the nature of cell-type specific expression of Ca<sub>v</sub>3.2 protein, we also investigated the distribution of Ca<sub>v</sub>3.2 mRNA using *in situ* hybridization.

Correspondence: Tao Liu, Center for Experimental Medicine, the First Affiliated Hospital of Nanchang University, 17 Yongwaizheng Street, Nanchang 3330006, China.  
Tel. +86.791.88692139 - Fax: +86.791.88692139.  
E-mail: liutao1241@ncu.edu.cn

Key words: Ca<sub>v</sub>3.2; immunohistochemistry; antigen retrieval; spinal dorsal horn.

Contributions: XEC, major experiments, manuscript drafting; LXM, XJF, MYZ, DYZ, LLX, experiment assistance, data analysis; TL, study concept, data interpretation, manuscript revision.

Conflict of interest: The authors declare no conflict of interest.

Funding: This work was supported by the National Natural Science Foundation of China (No. 31660289 to T.L. and 81560198 to D.Y.Z.) and the Outstanding Young People Foundation of Jiangxi Province (20171BCB23091).

Received for publication: 18 October 2018.  
Accepted for publication: 20 January 2019.

This work is licensed under a Creative Commons Attribution-NonCommercial 4.0 International License (CC BY-NC 4.0).

©Copyright X.E Cheng *et al.*, 2019  
Licensee PAGEPress, Italy  
European Journal of Histochemistry 2019; 63:2988  
doi:10.4081/ejh.2019.2988

Together, our results demonstrated that AR pre-treatment is essential for the IHC experiment of Ca<sub>v</sub>3.2 in SDH. These results may provide a theoretical basis for such kinds of experiments in the future.

### Materials and Methods

#### Animals

Sprague-Dawley (SD) rats (5-8 w) and wild type (WT) C57/BL6 mice (6-8 w) of either sex were obtained from the Animal Center of Nanchang University. Ca<sub>v</sub>3.2 knock-out (KO) mice (C57/BL6) were purchased from the Jackson Laboratory (Bar Harbor, ME, USA). Animals were housed in controlled room temperature (RT, 22-25°C) and maintained on a 12-h light/dark cycle with water and food *ad libitum*. All experimental procedures were approved by the Ethics Committee of Nanchang University.

#### Tissue collection and preparation

The rats and mice were deeply anesthetized by intraperitoneal injection of 1.5

g/kg urethane and perfused transcardially with saline followed by cold 4% paraformaldehyde (PFA) in 0.1 M phosphate buffer. The L4-L5 spinal cord segments were removed and post-fixed in 4% PFA for 6 h, and then cryoprotected in a 30% sucrose solution for 3 days. The L4 and L5 DRGs were post-fixed in 4% PFA for 6 h and cryoprotected in a 20% sucrose solution for 12 h. After embedding in optimal cutting temperature medium, 30  $\mu$ m (IHC staining) or 15  $\mu$ m (*in situ* hybridization) transverse spinal cord sections and 15  $\mu$ m DRG sections were prepared using a freezing microtome (CM1950, Leica, Nussloch, Germany).

### Immunostaining

All the spinal cord and DRG sections for IHC staining were first rinsed with 0.01 M phosphate-buffered saline (PBS) three times. Then they were divided into no-AR (without AR pre-treatment) or AR (with AR pre-treatment) groups. Sections in AR groups were subjected to heat-induced AR in a water bath (HH-2, China) at 98°C for 10 min by using 0.01 M sodium citrate buffer (pH 6.0, Solarbio) and were cooled to RT. Next, the free-floating sections were incubated in a blocking solution (0.3% Triton X-100, 1% albumin from bovine serum, and 1% normal donkey serum in PBS) for 30 min at RT to prevent nonspecific staining and then were incubated in a solution containing primary antibodies for three nights at 4°C. Primary antibodies used were rabbit anti-Ca<sub>v</sub>3.1-3.3 (1:200, Cat# ACC-021, Cat# ACC-025, Cat# ACC-009, Alomone), goat anti-Ca<sub>v</sub>3.2 (1:50, Cat# sc-16261, Santa Cruz), guinea pig anti-NeuN (1:200, Cat# 266004, Synaptic Systems), goat anti-GFAP (1:2000, Cat# ab53554, Abcam). After washing, the sections were incubated with appropriate secondary antibodies: donkey anti-rabbit Alexa Fluor 488 (1:400, Cat# A-21206, Invitrogen), donkey anti-goat Alexa Fluor 555 (1:400, Cat# A-21432, Invitrogen), donkey anti-guinea pig Cy5 (1:400, Cat# 706-175-148, Jackson ImmunoResearch) overnight at 4°C. After mounting the sections with Aqua-Poly/mount medium (Polysciences, Inc., Warrington, PA), they were observed under a Zeiss LSM700 confocal microscope (Germany) with ZEN 2010 software. The specificity of Ca<sub>v</sub>3.1-3.3 antibodies (Alomone) was tested by either omission or pre-absorption of primary antibodies with peptide antigens using sections with AR pre-treatment. Moreover, the specificity of anti-Ca<sub>v</sub>3.2 (Alomone) was also confirmed by the Ca<sub>v</sub>3.2 KO mice. Co-localization images of Ca<sub>v</sub>3.2 with other antibodies were taken with a 63x oil objective at a 0.5x zoom. The parameters for acquiring the

images, such as the number of recording pixels, electrical shutter speed, gain, and pinhole were kept unchanged throughout the whole experiment process. The quantification of co-localization was assessed by the ZEN 2010 software as our previous study.<sup>21</sup>

### *In situ* hybridization

The method for *in situ* hybridization was modified from a previous publication.<sup>15</sup> The Ca<sub>v</sub>3.2 probe (5'-ACAAUGCCAUCAAAGAUGUUGUAGGGGUUCCGAAUG-3') was designed for mouse *Cacna1h* gene (NM\_021415.4) and was labeled at 5'-end with digoxigenin. Briefly, spinal cord sections were treated with proteinase K (20  $\mu$ g/mL) for 20 min and fixed in 4% PFA for 15 min at RT. After that, the sections were rinsed with PBS containing 0.1% Tween-20 (PBST). Next, they were treated with 0.25% acetic anhydride in 0.1 M triethanolamine (pH 8.0) and rinsed with PBST three times. Following this, sections were incubated in pre-hybridization solution (50% formamide, 5  $\times$  SSC, 0.1% Tween-20, 0.3 mg/mL yeast tRNA, and 5  $\times$  Denhardt's Solution) for 4 h at 37°C, and then incubated in the hybridization solution (pre-hybridization solution plus digoxin-labeled probe) for 16 h at 37°C. After hybridization, the sections were washed three times with 2  $\times$  saline-sodium citrate, containing 0.1% Tween-20 (SSCT) at 37°C (15 min each) and one time with 1  $\times$  SSCT and 0.5  $\times$  SSCT at RT, respectively. Afterward, the sections were blocked with 0.5% sheep serum (Solarbio) for 1.5 h and incubated with alkaline phosphatase-conjugated anti-digoxigenin antibody (Roche Diagnostics) overnight at 4°C. Then they were incubated with a mixture of nitroblue tetrazolium chloride (NBT, Sangon Biotech) and 5-bromo-4-chloro-3-indolylphosphate (BCIP, Sangon Biotech) for 1~3 h for color development. In addition, to compare the results of the *in situ* hybridization with that of the IHC, partial sections were further incubated with anti-Ca<sub>v</sub>3.2 (Alomone) and GFAP as well as 4',6-Diamidino-2-Phenylindole (DAPI, 1:1000, Cat# D9542, Sigma, sections were incubated with DAPI for 10 min at RT before mounting) and were visualized by an FSX100 microscope equipped with a digital camera system (Olympus, Japan) or the Zeiss LSM700 confocal microscope.

### Statistical analysis

SPSS version 17.0 (SPSS Inc, Chicago, IL, USA) was used for statistical analysis. All data are expressed as mean  $\pm$  SEM. Shapiro-Wilk test was used to assess the normality of data. Differences between groups were compared using unpaired

Student's *t*-test.  $P < 0.05$  was considered statistically significant.

## Results

### Immunolabeling of Ca<sub>v</sub>3 isoforms in SDH and DRG of SD rats with or without AR pre-treatment

Although the distributions of Ca<sub>v</sub>3.1, Ca<sub>v</sub>3.2, and Ca<sub>v</sub>3.3 mRNAs have been identified in both SDH and DRG,<sup>2</sup> IHC studies in these areas were mostly focused on Ca<sub>v</sub>3.2. However, hyperalgesia could also be observed in Ca<sub>v</sub>3.1 null mice,<sup>22</sup> suggesting Ca<sub>v</sub>3.1 might contribute to the sensory perception of pain as well. Therefore, we first investigated the expression of Ca<sub>v</sub>3.1, Ca<sub>v</sub>3.2, and Ca<sub>v</sub>3.3 isoforms in SDH and DRG with or without AR pre-treatment. As shown in Figure 1, regardless of whether sections were processed with (right) or without (left) AR, Ca<sub>v</sub>3.1-immunoreactivity (IR) showed a punctate staining pattern in SDH (Figure 1 A,D) and Ca<sub>v</sub>3.3-IR was primarily distributed around the neuron-like membranes (Figure 1 C,F). However, we found a significantly different expression pattern of Ca<sub>v</sub>3.2-IR in sections processed with AR from those without AR pre-treatment. For sections lacking AR pre-treatment, Ca<sub>v</sub>3.2-IR showed a glial cell-like appearance (Figure 1B), which is similar to the results of Li *et al.*<sup>9</sup> However, for those sections with AR pre-treatment, Ca<sub>v</sub>3.2-IR showed a neuron-like appearance (Figure 1E), which was in line with the findings of Chen *et al.*<sup>5</sup> Next, we investigated whether AR-caused different IHC staining exists in other tissues, such as DRG, which is mostly studied for the mechanisms of pain. As shown in Figure 1 G-L, Ca<sub>v</sub>3.1, Ca<sub>v</sub>3.2, and Ca<sub>v</sub>3.3-IR were highly expressed at neuron-like membranes and cytoplasm. In addition, unlike the observations of Ca<sub>v</sub>3.2-IR in SDH, AR pre-treatment did not affect the expression pattern of Ca<sub>v</sub>3.2 in DRG. Together, these findings demonstrate that AR pre-treatment altered the IHC staining results of Ca<sub>v</sub>3.2 in rat SDH but not DRG, without any effect on Ca<sub>v</sub>3.1 and Ca<sub>v</sub>3.3 isoforms.

### Immunolabeling of Ca<sub>v</sub>3 isoforms in SDH and DRG of mice with or without AR pre-treatment

Since the Ca<sub>v</sub>3.2-IR showed a different IHC staining pattern in rat SDH, we wonder whether this difference is due to the species of animal. Besides rat, mouse is the most commonly used animal species. Therefore, we next performed the same experiment on mice SDH. We found that Ca<sub>v</sub>3.1- (Figure 2 A,D) and Ca<sub>v</sub>3.3-IR (Figure 2 C,F) were

similar in mice SDH sections with or without AR pre-treatment. However, the results of  $Ca_v3.2$ -IR (Figure 2 B,E) were affected by AR pre-treatment, which is highly similar to that of the rats. AR pre-treatment led to the  $Ca_v3.2$ -IR exhibited a neuron-like appearance in mice SDH, too. However, no differences of  $Ca_v3.1$ - and  $Ca_v3.3$ -IR in SDH from both rat and mouse were observed whether pre-treated with AR or not.

### Discrepancies of $Ca_v3.2$ -IR from two different sources of antibodies with or without AR pre-treatment

Anti- $Ca_v3.1$ - $Ca_v3.3$  antibodies used in the above study were all from the Alomone Company. We were curious whether the different results of  $Ca_v3.2$ -IR in SDH would have been the same if an alternative commercial anti- $Ca_v3.2$  antibody was used.

Therefore, we next compared the  $Ca_v3.2$ -IR in SDH by using two different commercial sources of anti- $Ca_v3.2$  (Alomone vs Santa Cruz). As shown in Figure 3 A-C, without AR pre-treatment, the IR of the two sources of  $Ca_v3.2$  antibodies were similar in rat SDH sections, which both showed a glial cell-like appearance and a substantial colocalization. However, for those sections with AR pre-treatment, the IR of anti- $Ca_v3.2$  antibody from Alomone was mostly expressed in neuron-like cells (Figure 3D), while there was no change for the IR of anti- $Ca_v3.2$  antibody from Santa Cruz which still shows a glial cell-like appearance (Figure 3E). Furthermore, after pre-treating with AR, the extent of co-staining was significantly decreased (Figure 3F). These data suggested that AR pre-treatment

has a different effect on  $Ca_v3.2$ -IR from various commercial sources of antibodies.

### Co-localization of $Ca_v3.2$ with GFAP and NeuN in sections of SDH pre-treated with AR or not

Above results suggested that immunostaining of  $Ca_v3.2$  (Alomone) has neuron-like and glial-cell like appearances with or without AR pre-treatment, respectively. To further confirm the cell-type specific expression of  $Ca_v3.2$ , we next co-stained  $Ca_v3.2$  with GFAP and NeuN. As shown in Figure 4A-E, it is clear that without AR pre-treatment,  $Ca_v3.2$  was largely co-stained with GFAP but not NeuN. In contrast, with AR pre-treatment,  $Ca_v3.2$  was major co-stained with NeuN but not GFAP (Figure 4F-J). Quantitative analysis (Figure 4K) demonstrated that the co-localized ratio of  $Ca_v3.2$

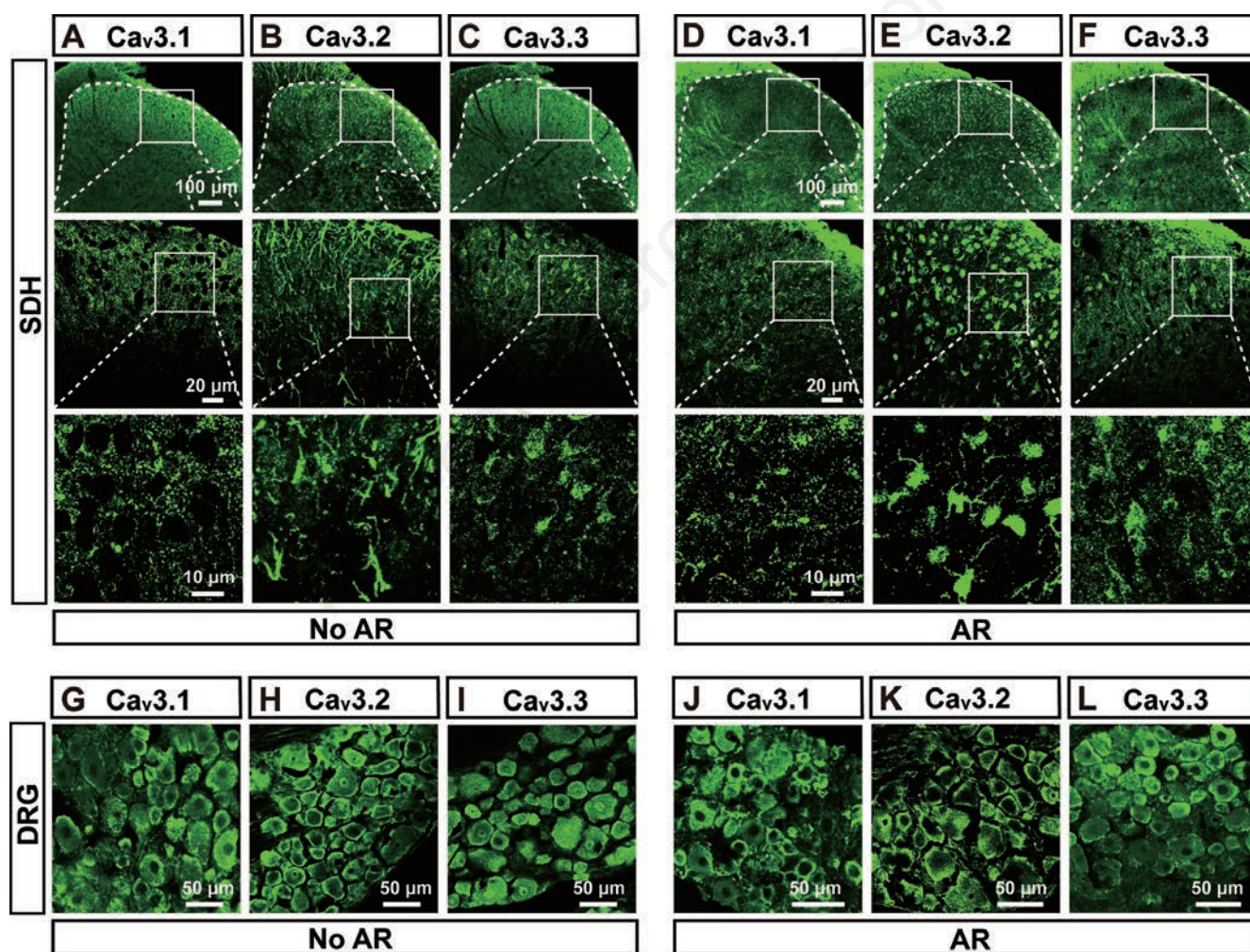


**Figure 1.** Expression of  $Ca_v3.1$ - $3.3$  isoforms (Alomone) in SDH and DRG of SD rats with or without AR pre-treatment. Representative confocal images of  $Ca_v3.1$  (A),  $Ca_v3.2$  (B), and  $Ca_v3.3$  (C) in SDH without AR pre-treatment (No AR). Representative confocal images of  $Ca_v3.1$  (D),  $Ca_v3.2$  (E), and  $Ca_v3.3$  (F) in SDH with AR pre-treatment (AR). Representative images of  $Ca_v3.1$  (G),  $Ca_v3.2$  (H), and  $Ca_v3.3$  (I) in DRG without AR pre-treatment (No AR). Representative images of  $Ca_v3.1$  (J),  $Ca_v3.2$  (K), and  $Ca_v3.3$  (L) in DRG with AR pre-treatment (AR).

## Mouse SDH

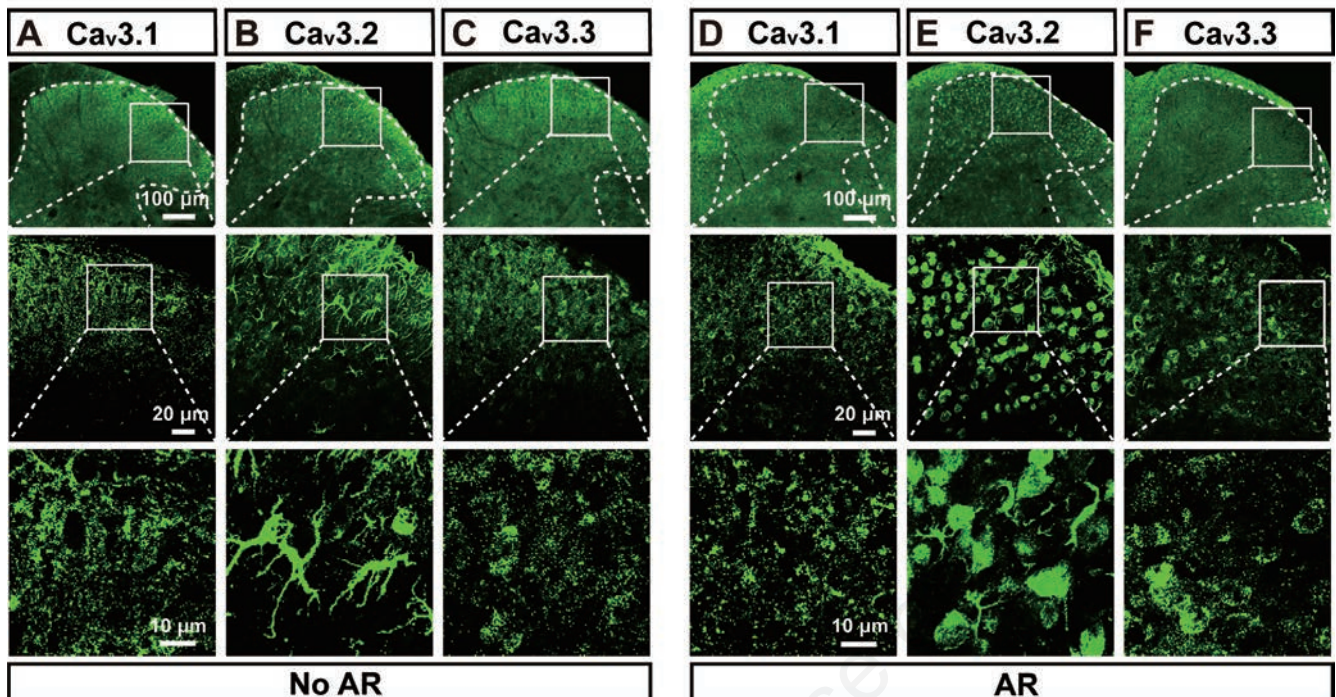


Figure 2. Expression of Cav3.1-3.3 isoforms (Alomone) in mice SDH sections pre-treated with AR or not. Representative images of Cav3.1 (A), Cav3.2 (B), and Cav3.3 (C) in SDH without AR pre-treatment (no AR). Representative images of Cav3.1 (D), Cav3.2 (E), and Cav3.3 (F) in SDH with AR pre-treatment (AR).

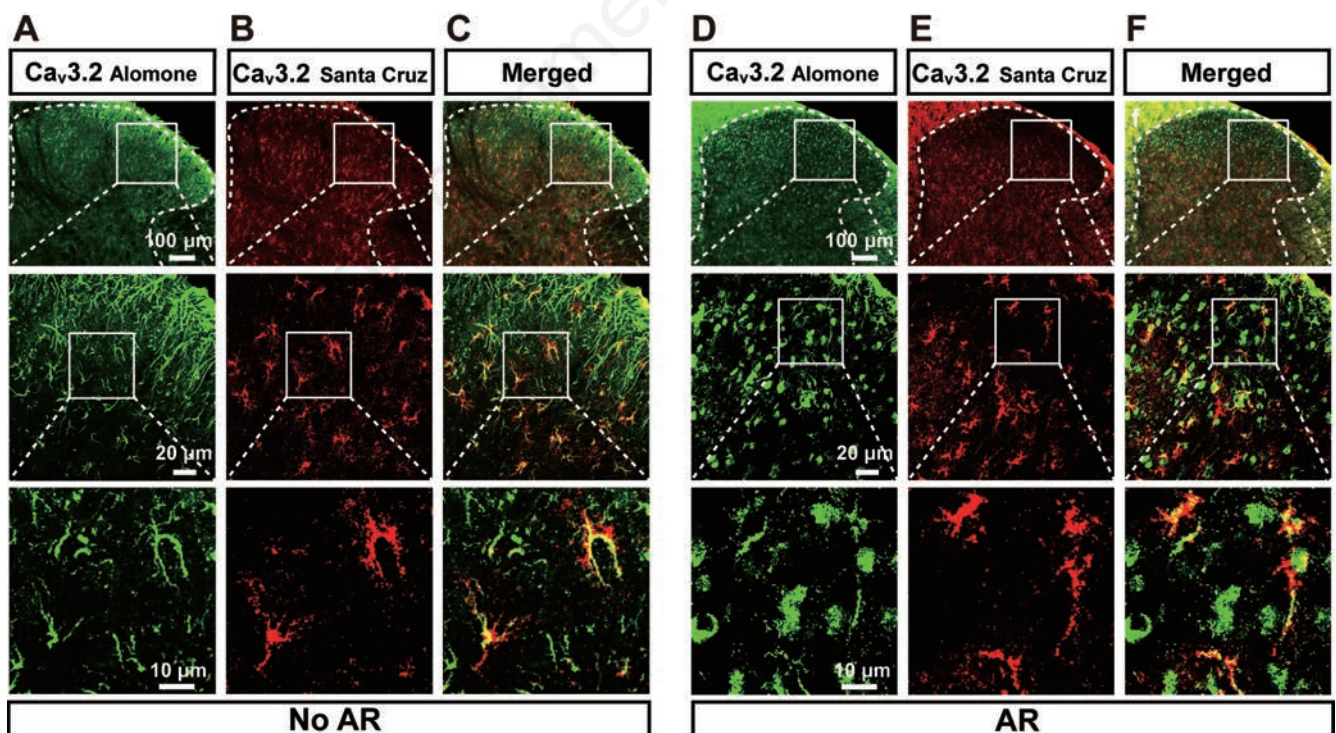


Figure 3. Expression of anti- Cav3.2 from two companies in rat SDH with or without AR pre-treatment. A) Representative image of Cav3.2 (Alomone, green) in SDH without AR pre-treatment (No AR). B) Representative image of Cav3.2 (Santa Cruz, red) in SDH without AR pre-treatment (No AR). C) Merged images of (A) and (B). D) Representative image of Cav3.2 (Alomone, green) in SDH with AR pre-treatment (AR). E) Representative image of Cav3.2 (Santa Cruz, red) in SDH with AR pre-treatment (AR). F) Merged images of (D) and (E).

with GFAP in sections without AR pre-treatment was higher ( $30.4 \pm 4.4\%$  vs  $9.4 \pm 0.4\%$ ,  $n=7$ ,  $P<0.01$ ) than that of the sections pre-treated with AR. The results for the co-localization of Ca<sub>v</sub>3.2 with NeuN were *vice versa* ( $12.4 \pm 0.7\%$  vs  $28.2 \pm 1.3\%$ ,  $n=7$ ,  $P<0.001$ ). In control experiments by omitting the primary antibodies or pre-absorbing the primary antibodies with peptide antigens, no IHC signal was detected (Supplementary Figures 1 and 2). Moreover, we tested the specificity of Ca<sub>v</sub>3.2 antibody (Alomone) by using the SDH sections with AR pre-treatment from WT and Ca<sub>v</sub>3.2 KO mice. Strong Ca<sub>v</sub>3.2-IR

was observed in SDH of WT mice (Figure 4L) but not Ca<sub>v</sub>3.2 KO mice (Figure 4M), which demonstrated the specificity of Ca<sub>v</sub>3.2 antibody (Alomone). Furthermore, western blotting using SDH tissues from mice implied that Ca<sub>v</sub>3.2 (Alomone) is expressed in WT mouse rather than KO mouse, suggesting its fine specificity for western blot (Supplementary Figure 3). Together, these results suggested that AR pre-treatment caused the co-localization of Ca<sub>v</sub>3.2 shifted from GFAP to NeuN.

To identify the nature distribution pattern of Ca<sub>v</sub>3.2, we next performed the *in situ*

hybridization experiment to study the expression of Ca<sub>v</sub>3.2 mRNA, which showed that the Ca<sub>v</sub>3.2 mRNA positive stain cells have a neuron-like appearance (Figure 5A). The sections of *in situ* hybridization were further processed to IHC co-stain for Ca<sub>v</sub>3.2, GFAP, and DAPI. Figure 5 B-G showed that most of the Ca<sub>v</sub>3.2 mRNA positive cells are also anti-Ca<sub>v</sub>3.2-positive but not GFAP-positive cells. For conclusion, these results demonstrated that the expression pattern of Ca<sub>v</sub>3.2-IR with AR pre-treatment is closer to that of Ca<sub>v</sub>3.2 mRNA, suggesting that the Ca<sub>v</sub>3.2 positive cells should be neurons but not astrocytes.

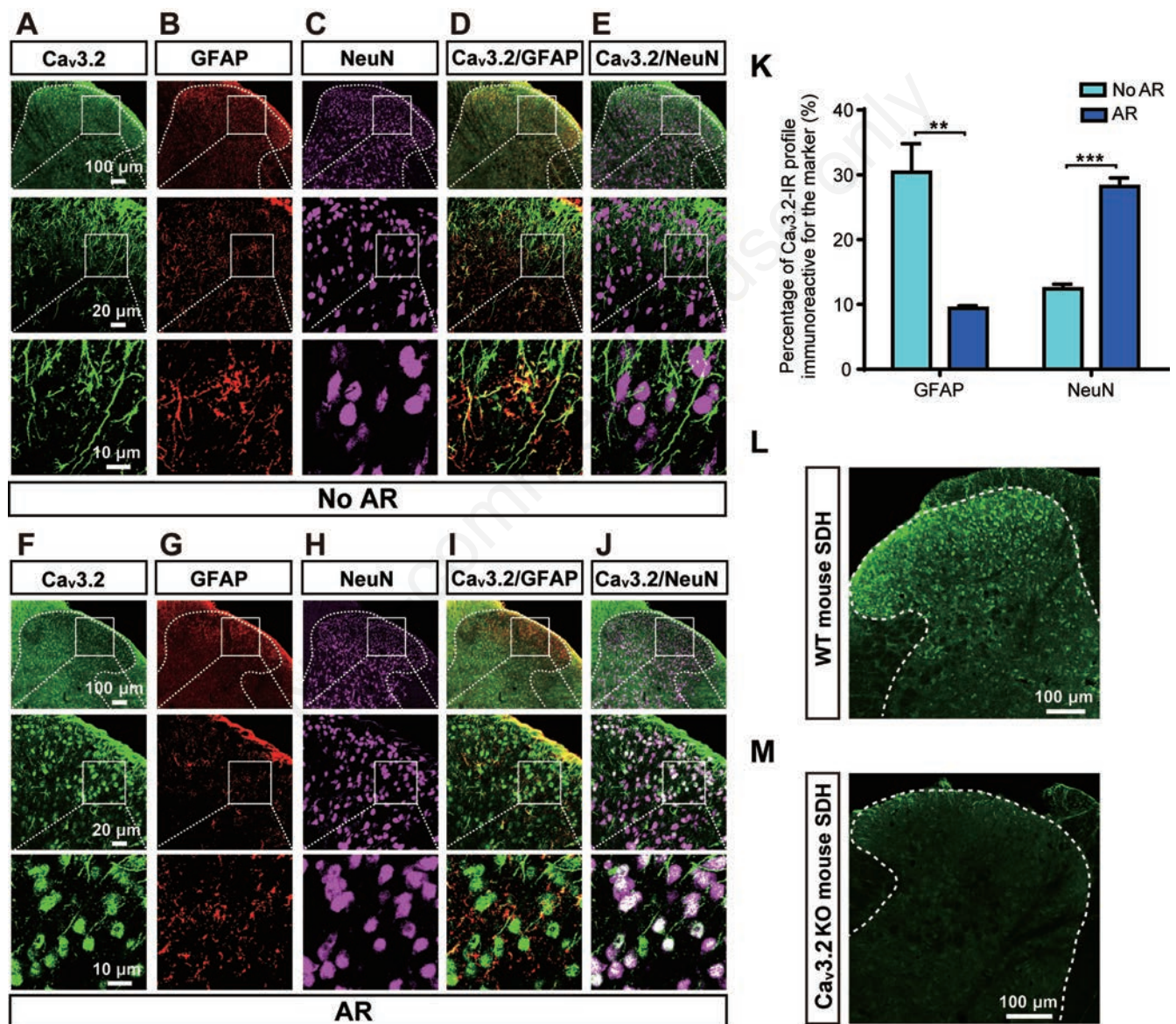


**Figure 4.** Expression pattern of Ca<sub>v</sub>3.2 (Alomone) in rat SDH with or without AR pre-treatment. Representative images of Ca<sub>v</sub>3.2 (A, green), GFAP (B, red), NeuN (C, magenta), merged images of Ca<sub>v</sub>3.2 and GFAP (D), and merged images of Ca<sub>v</sub>3.2 and NeuN (E) in SDH without AR pre-treatment (No AR). Representative images of Ca<sub>v</sub>3.2 (F, green), GFAP (G, red), NeuN (H, magenta), merged images of Ca<sub>v</sub>3.2 and GFAP (I), and merged images of Ca<sub>v</sub>3.2 and NeuN (J) in SDH with AR pre-treatment (AR). K Quantitative colocalization results of Ca<sub>v</sub>3.2-IR with NeuN- and GFAP-IR. Representative images of Ca<sub>v</sub>3.2 (Alomone) in SDH from wild-type mice (L) and Ca<sub>v</sub>3.2 knock-out (KO) mice (M). \*\* $P<0.01$ , \*\*\* $P<0.001$ .

## Discussion

The immunohistochemistry technique is used to detect cell or tissue antigens.<sup>23</sup> Principal factors affecting the outcome of IHC studies include the following: i) tissue fixation and processing, ii) unmasking of

epitopes, and iii) sensitivity of the detection system.<sup>24</sup> Formaldehyde is one of the most popular fixatives due to its low cost, ease of preparation, and because of its well morphologic detail with few artifacts. However, formaldehyde fixation could mask or damage some binding sites of antibodies, which

might lead to the loss of IR.<sup>25,26</sup> AR pre-treatment, which is mainly based on high-temperature heating of tissues, is an effective method to overcome these disadvantages.<sup>27,28</sup> Since 2007, genetic linkage studies have implicated *Ca<sub>v</sub>3.2* gene coded protein as a pain modulation related protein.

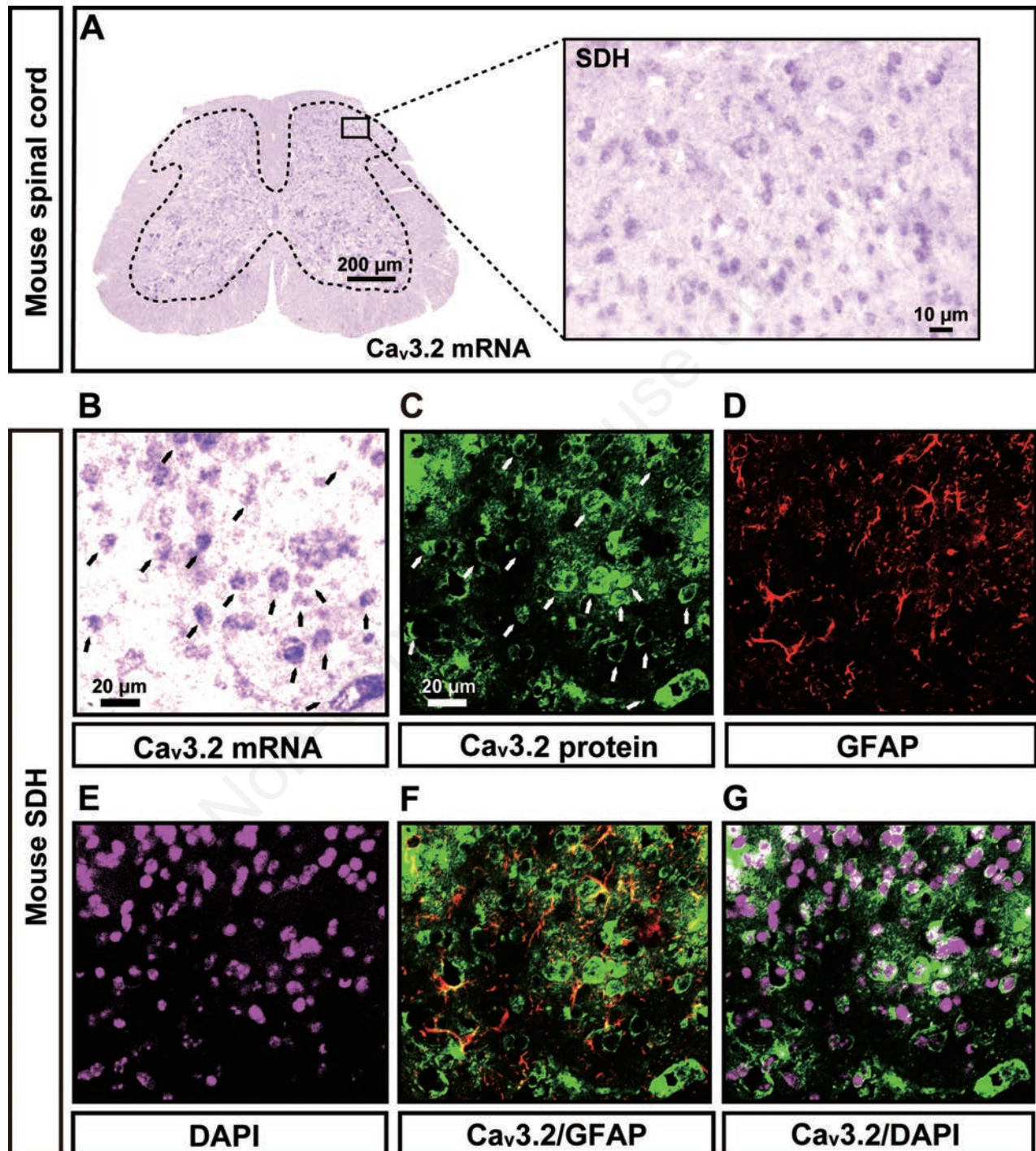


Figure 5. Expression pattern of *Ca<sub>v</sub>3.2* mRNA in mouse SDH. A) Microscopic images of a DIG-labeled *Ca<sub>v</sub>3.2* probe for *in situ* hybridization in mice SDH. Triple-labeling of *in situ* hybridization sections for *Ca<sub>v</sub>3.2* mRNA (B, purple) and the following IHC staining of *Ca<sub>v</sub>3.2* (C, green, Alomone), GFAP (D, red), DAPI (E, magenta), merged images of *Ca<sub>v</sub>3.2* and GFAP (F), and merged images of *Ca<sub>v</sub>3.2* and DAPI (G). Note that *Ca<sub>v</sub>3.2* mRNA is expressed in *Ca<sub>v</sub>3.2*-positive cells (arrows) but not GFAP-positive astrocytes.

However, there were disagreements as to the expression pattern of Ca<sub>v</sub>3.2 in SDH of SD rat.<sup>5,9</sup> We therefore raised the hypothesis that AR pre-treatment might account for this difference. To test this hypothesis, we observed the effect of AR pre-treatment on IHC staining of Ca<sub>v</sub>3.1-3.3 in rat SDH and DRG as well as mouse SDH.

Ca<sub>v</sub>3 channels can be activated around resting membrane potential and are inactivated within a few tens of milliseconds.<sup>29</sup> Hence, they are also known as transiently open calcium channels. In the nervous system, Ca<sub>v</sub>3 channels are involved in the regulation of neuronal excitability, thus they are linked to the pathogenesis of various neurological disorders, including chronic pain. In multiple animal models of neuropathic pain, Ca<sub>v</sub>3 was upregulated in DRG and SDH.<sup>30-32</sup> Among the three Ca<sub>v</sub>3 isoforms, Ca<sub>v</sub>3.2 is the most concerned subtype with neuropathic pain.<sup>12</sup> Consistent with previous studies showing that Ca<sub>v</sub>3.2 was mainly distributed in small- to medium-sized DRG neurons,<sup>14,15</sup> our data found that Ca<sub>v</sub>3.2, as well as Ca<sub>v</sub>3.1 and Ca<sub>v</sub>3.3, had similar expression pattern in DRG with or without AR pre-treatment. Interestingly, previous studies showed that the distribution pattern of Ca<sub>v</sub>3.2 in SDH is controversial. Chen *et al.* found that, in L5/6 spinal nerve ligation pain model, the expression of Ca<sub>v</sub>3.2 (Santa Cruz, rabbit) in SDH of SD rats was upregulated seven days after nerve ligation.<sup>5</sup> Moreover, they found that Ca<sub>v</sub>3.2 is expressed in neurons (co-localize with NeuN) but not astrocytes (co-localize with GFAP). However, in SDH of SD rats suffered from paclitaxel-induced peripheral neuropathy, the Ca<sub>v</sub>3.2 (Alomone, rabbit) expression was increased and co-localized to GFAP positive but not NeuN positive cells.<sup>9</sup> These distinct results may be due to the antibodies they used were from different companies. Thus, we investigated the Ca<sub>v</sub>3.2 expression in SDH of SD rats with the antibodies from the above two companies. Differently from Chen *et al.*'s study (Santa Cruz - rabbit),<sup>5</sup> our results found that Ca<sub>v</sub>3.2-IR from Santa Cruz (goat) showed a glia-like appearance and was irrelevant to AR pre-treatment. This difference might be due to the different sourced anti-Ca<sub>v</sub>3.2. However, Santa Cruz does not provide rabbit-sourced Ca<sub>v</sub>3.2 which is out of the market. Currently, only a mouse-sourced Ca<sub>v</sub>3.2 is available. Therefore, we performed the IHC staining of Ca<sub>v</sub>3.2 using a rabbit-sourced anti-Ca<sub>v</sub>3.2 (C1868) from Sigma-Aldrich (*data not shown*). Whereas, the Ca<sub>v</sub>3.2-IR (Sigma-Aldrich) displayed a punctate staining with or without AR pre-treatment, suggesting the source of Ca<sub>v</sub>3.2 has little effect on Ca<sub>v</sub>3.2-IR. In contrast, AR pre-treatment influenced the results of

Ca<sub>v</sub>3.2-IR from Alomone (rabbit). Our triple-labeling experiments found that Ca<sub>v</sub>3.2 (Alomone) was co-localized with NeuN but not GFAP after AR pre-treatment, further demonstrating that AR pre-treatment impacts the results of Ca<sub>v</sub>3.2-IR in SDH.

Given that mice are also the commonly used rodents for pain animal models, we next observed the effect of AR on Ca<sub>v</sub>3.2 (Alomone) on SDH sections from mouse and got the same results. A recent study demonstrated that Ca<sub>v</sub>3.2 was co-stained with PKCγ-containing interneurons in the Ca<sub>v</sub>3.2-GFP knock-in mice, suggesting Ca<sub>v</sub>3.2 is expressed in neurons.<sup>6</sup> In line with this study, our IHC results of Ca<sub>v</sub>3.2-IR in mice showed that under the pre-treatment of AR, Ca<sub>v</sub>3.2-IR displayed the neuron-like appearance.

Although one previous report described Ca<sub>v</sub>3.2 (α1H) mRNA was mostly expressed in the outermost layers (layers 1-2) of SDH,<sup>2</sup> our present findings indicate that Ca<sub>v</sub>3.2 mRNA is present throughout the gray matter of spinal cord. Since the sections for *in situ* hybridization included sodium citrate and heat pre-treatment, post-IHC of Ca<sub>v</sub>3.2 protein (Alomone) from *in situ* hybridization sections largely matched the distribution of Ca<sub>v</sub>3.2 mRNA. Furthermore, our and previous electrophysiological studies have revealed the presence of T-type channels in SDH neurons,<sup>33-35</sup> which highly suggested that Ca<sub>v</sub>3.2 is expressed in neurons. These data suggested that AR pre-treatment might be necessary for specific antigens, including Ca<sub>v</sub>3.2.

Taken together, we have demonstrated that AR pre-treatment affect the Ca<sub>v</sub>3.2-IR in rat and mouse SDH and we believe that our findings make a significant contribution to the future research of Ca<sub>v</sub>3.2 distribution in SDH from both rats and mice.

## References

1. Perez-Reyes E. Molecular physiology of low-voltage-activated t-type calcium channels. *Physiol Rev* 2003;83:117-61.
2. Talley EM, Cribbs LL, Lee JH, Daud A, Perezreyes E, Bayliss DA. Differential distribution of three members of a gene family encoding low voltage-activated (T-type) calcium channels. *J Neurosci* 1999;19:1895-911.
3. McKay BE, Mcrory JE, Molineux ML, Hamid J, Snutch TP, Zamponi GW, et al. CaV3 T-type calcium channel isoforms differentially distribute to somatic and dendritic compartments in rat central neurons. *Eur J Neurosci* 2006; 24:2581-94.
4. Jacus MO, Uebele VN, Renger JJ, Todorovic SM. Presynaptic CaV3.2

channels regulate excitatory neurotransmission in nociceptive dorsal horn neurons. *J Neurosci* 2012;32:9374-82.

5. Chen YL, Tsaor ML, Wang SW, Wang TY, Hung YC, Lin CS, et al. Chronic intrathecal infusion of mibefradil, ethosuximide and nickel attenuates nerve ligation-induced pain in rats. *Br J Anaesth* 2015;115:105-11.
6. François A, Schüetter N, Laffray S, Sanguesa J, Pizzoccaro A, Dubel S, et al. The low-threshold calcium channel Cav3.2 determines low-threshold mechanoreceptor function. *Cell Rep* 2015;10:370-82.
7. Aguado C, García-Madrona S, Gil-Mínguez M, Luján R. Ontogenic changes and differential localization of T-type Ca(2+) channel subunits Cav3.1 and Cav3.2 in mouse hippocampus and cerebellum. *Front Neuroanat* 2016; 10:83.
8. Ozaki T, Matsuoka J, Tsubota M, Tomita S, Sekiguchi F, Minami T, et al. Zinc deficiency promotes cystitis-related bladder pain by enhancing function and expression of Cav3.2 in mice. *Toxicology* 2018;393:102-12.
9. Li Y, Tatsui CE, Rhines LD, North RY, Harrison DS, Cassidy RM, et al. Dorsal root ganglion neurons become hyperexcitable and increase expression of voltage-gated T-type calcium channels (Cav3.2) in paclitaxel-induced peripheral neuropathy. *Pain* 2017;158:417-29.
10. García-Caballero A, Gadotti V, Stenkowski P, Weiss N, Souza I, Hodgkinson V, et al. The deubiquitinating enzyme USP5 modulates neuropathic and inflammatory pain by enhancing CaV3.2 channel activity. *Neuron* 2014;83:1144-58.
11. Zamponi GW, Striessnig J, Koschak A, Dolphin AC. The physiology, pathology, and pharmacology of voltage-gated calcium channels and their future therapeutic potential. *Pharmacol Rev* 2015;67:821-70.
12. Bourinet E, Alloui A, Monteil A, Barrère C, Couette B, Poirot O, et al. Silencing of the Cav3.2 T-type calcium channel gene in sensory neurons demonstrates its major role in nociception. *EMBO J* 2005;24:315-24.
13. Shiue SJ, Wang CH, Wang TY, Chen YC, Cheng JK. Chronic intrathecal infusion of T-type calcium channel blockers attenuates CaV3.2 upregulation in nerve-ligated rats. *Acta Anaesthesiol Taiwan* 2016;54: 81-7.
14. Rose KE, Lunardi N, Boscolo A, Dong X, Erisir A, Jevtovic-Todorovic V, et al. Immunohistological demonstration of CaV3.2 T-type voltage-gated calcium channel expression in soma of dorsal

- root ganglion neurons and peripheral axons of rat and mouse. *Neuroscience* 2013;250:263-74.
15. Watanabe M, Ueda T, Shibata Y, Kumamoto N, Shimada S, Ugawa S. Expression and regulation of Cav3.2 T-Type calcium channels during inflammatory hyperalgesia in mouse dorsal root ganglion neurons. *PLoS One* 2015; 10:e0127572.
  16. Lin SF, Yu XL, Liu XY, Wang B, Li CH, Sun YG, et al. Expression patterns of T-type Cav3.2 channel and insulin-like growth factor-1 receptor in dorsal root ganglion neurons of mice after sciatic nerve axotomy. *Neuroreport* 2016;27: 1174-81.
  17. Liu Q-Y, Chen W, Cui S, Liao F-F, Yi M, Liu F-Y, et al. Upregulation of Cav3.2 T-type calcium channels in adjacent intact L4 dorsal root ganglion neurons in neuropathic pain rats with L5 spinal nerve ligation. *Neurosci Res* 2018.
  18. Zhang Y, Qin W, Qian Z, Liu X, Wang H, Gong S, et al. Peripheral pain is enhanced by insulin-like growth factor 1 through a G protein-mediated stimulation of T-type calcium channels. *Sci Signal* 2014;7:ra94.
  19. Dapson RW. Macromolecular changes caused by formalin fixation and antigen retrieval. *Biotech Histochem* 2009;82: 133-40.
  20. Gown AM. Unmasking the mysteries of antigen or epitope retrieval and formalin fixation. *Am J Clin Pathol* 2004;121: 172-4.
  21. Peng SC, Wu J, Zhang DY, Jiang CY, Xie CN, Liu T. Contribution of presynaptic HCN channels to excitatory inputs of spinal substantia gelatinosa neurons. *Neuroscience* 2017;358:146-57.
  22. Kim D, Park D, Choi S, Lee S, Sun M, Kim C, et al. Thalamic control of visceral nociception mediated by T-type Ca<sup>2+</sup> channels. *Science* 2003;302:117-9.
  23. Brandtzaeg P. The increasing power of immunohistochemistry and immunocytochemistry. *J Immunol Methods* 1998;216:49-67.
  24. Werner M, Wasielewski RV, Komminoth P. Antigen retrieval, signal amplification and intensification in immunohistochemistry. *Histochem Cell Biol* 1996;105:253-60.
  25. French D, Edsall JT. The reactions of formaldehyde with amino acids and proteins. *Adv Protein Chem* 1945;2: 277-35.
  26. Helander KG. Kinetic studies of formaldehyde binding in tissue. *Stain Technol* 1994;69:177-9.
  27. Hayashi T, Lewis A, Hayashi E, Betenbaugh MJ, Su TP. Antigen retrieval to improve the immunocytochemistry detection of sigma-1 receptors and ER chaperones. *Histochem Cell Biol* 2011;135:627-37.
  28. Hussaini SM, Jun H, Cho CH, Kim HJ, Kim WR, Jang MH. Heat-induced antigen retrieval: an effective method to detect and identify progenitor cell types during adult hippocampal neurogenesis. *J Vis Exp* 2013;78:e50769.
  29. Senatore A, Guan W, Spafford JD. Cav3 T-type channels: regulators for gating, membrane expression, and cation selectivity. *Pflugers Arch* 2014;466:645-60.
  30. Takahashi T, Aoki Y, Okubo K, Maeda Y, Sekiguchi F, Mitani K, et al. Upregulation of Ca(v)3.2 T-type calcium channels targeted by endogenous hydrogen sulfide contributes to maintenance of neuropathic pain. *Pain* 2010;150:183-91.
  31. Yue J, Liu L, Liu Z, Shu B, Zhang Y. Upregulation of T-type Ca<sup>2+</sup> channels in primary sensory neurons in spinal nerve injury. *Spine* 2013;38:463-70.
  32. Lai CY, Hsieh MC, Ho YC, Lee AS, Wang HH, Cheng JK, et al. Growth arrest and DNA-damage-inducible protein 45beta-mediated DNA demethylation of voltage-dependent T-type calcium channel 3.2 Subunit enhances neuropathic allodynia after nerve injury in rats. *Anesthesiology* 2017;126:1077-95.
  33. Ku WH, Schneider SP. Multiple T-type Ca<sup>2+</sup> current subtypes in electrophysiologically characterized hamster dorsal horn neurons: possible role in spinal sensory integration. *J Neurophysiol* 2011;106:2486-98.
  34. Ryu PD, Randic M. Low- and high-voltage-activated calcium currents in rat spinal dorsal horn neurons. *J Neurophysiol* 1990;63:273-85.
  35. Wu J, Peng S, Xiao L, Cheng X, Kuang H, Zhu M, et al. Cell-type specific distribution of T-type calcium currents in lamina II neurons of the rat spinal cord. *Front Cell Neurosci* 2018;12:370.